

Vehicular Link Performance: From Real-World Experiments to Reliability Models and Performance Analysis

Veronika Shivaldova^{*†}, Andreas Winkelbauer^{*}, Christoph F. Mecklenbräuer^{*†}

^{*}Institute of Telecommunications, Vienna University of Technology

[†]Christian Doppler Laboratory for Wireless Technologies for Sustainable Mobility, Vienna University of Technology
Gusshausstrasse 25/389, 1040 Vienna, Austria

email: {veronika.shivaldova, andreas.winkelbauer, christoph.mecklenbraeuer}@tuwien.ac.at

Abstract—Aiming at improvements in traffic safety and efficiency, dependable infrastructure-to-vehicle (V2I) communication links for intelligent transportation systems require an adequate deployment of roadside units (RSU). However, evaluating the dependence of key system performance indicators on RSU deployment conditions through field tests is expensive, especially for scenarios with large numbers of test vehicles. Therefore, numerous studies have been performed using network simulators that abstract the physical layer details. In this context we propose a range-dependent hidden Markov model (HMM), whose parameters are estimated from real-world IEEE 802.11p V2I measurements. The resulting packet error model is computationally inexpensive and incorporates the physical layer characteristics and propagation effects of an authentic highway environment with realistic vehicular traffic patterns. The influence of data rates, packet lengths, operational modes, and RSU antenna characteristics on coverage range and throughput is investigated based on model-generated simulation traces. We advertise this range-dependent HMM for future use in system-level performance evaluations of intelligent transportation systems. To this end, the model parameters are openly released to the research community.

I. INTRODUCTION

The enormous potential of cooperative vehicular systems to improve traffic safety and efficiency by means of wireless information exchange among vehicles, as well as between vehicles and infrastructure has been a research focus since the early 1990s. Significant evolution of this technology has prompted standardization bodies and automotive industry stakeholders worldwide to draw particular attention to its deployment and development. Since the efficient deployment is essential for the success of such cooperative systems, a deep understanding of the influence of every component and parameter is required to carry out practical design.

Influence of system components and parameters on system performance has been reported by several research groups based on empirical measurement campaigns. In [1], IEEE 802.11p-based vehicle-to-vehicle (V2V) communication performance was analyzed for various road configurations, such as straight sections, curves, and non-flat sections. The effect of objects obstructing the line-of-sight (LOS) on the V2V

communication range was analyzed in parking lot, highway, sub-urban and urban scenarios in [2]. V2V communication performance was evaluated in highway tunnel environments for various propagation conditions and overtaking maneuvers in [3].

In the infrastructure-to-vehicle (V2I) domain, the authors of [4] analyzed the communication performance for various transmission parameters in highway scenarios. The performance of V2I communications in urban environments was analyzed in terms of round-trip times, transaction times, and jitter in [5]. The authors of [6] observed a negligible influence of the vehicle velocity on the communication range for different data rates and packet lengths.

A significant part of the measurement-based research activities in the field of V2I communications considers the effects introduced by system components and operational modes. With regard to on-board unit (OBU) antennas, the authors of [7] have concluded that a rooftop position yields the best performance in terms of error rate. Addressing the effects introduced by the antenna positioning related to the road geometry, the authors of [8] have shown that system efficiency can be greatly enhanced by mounting roadside unit (RSU) antennas above all driving vehicles. Further field tests investigating the impact of operating and propagation conditions on IEEE 802.11p-based ad-hoc network performance were presented in [9].

However, the two types of experiments, the ones examining system parameters and the ones considering system components have rarely been combined. Therefore, the main objective of the field study presented here was to analyze the joint influence of different system parameters and components. To this end, an extensive measurement campaign has been carried out on the Austrian highway S1 during September 2010, within the ROADS SAFE project [10]. The performance of V2I communication was analyzed using 12 different setups, including three combinations of data rates and packet lengths, four RSU antenna types, two RSU mounting positions, and two driving directions.

In order to make the results of this V2I measurement

campaign accessible to the research community, we introduce a computationally inexpensive packet error model. Given a limited set of model parameters, available online under a non-commercial academic use license [11], model-generated packet error traces can be easily simulated. We suggest using the range-dependent packet error trace generator as an alternative physical layer abstraction in system-level simulation tools.

II. MODELING APPROACH

Markov chains are powerful and commonly used tools for modeling error statistics of communication channels. It consists of a finite number of states and corresponding state transition probabilities. The transition from one state to another is governed by the transition probabilities and takes place every time instant. The Markov chain can only be in one state at a time and the produced sample depends deterministically on this state. If, however, the samples depend on the states probabilistically, the states are hidden since they cannot be directly observed from the samples. Such models are called hidden Markov models (HMMs). The availability of efficient algorithms for the estimation of HMM parameters from experimental data makes their application in the field of vehicular communications simple and very beneficial. Given a set of suitable HMMs, performance analysis can be carried out on a computer which is cheap compared to highly expensive field tests. Moreover applying HMMs to model and reproduce real-world performance studies would create a valuable cross-layer interface between network layer and physical layer simulators, substantially improving the usefulness of existing simulators such as NS-3 and QualNet.

The statistical modeling of communication channels using HMMs goes back to the work of Gilbert in the 1960s. In [12], he proposed a simple first-order HMM with two states, called good and bad, as shown in Fig. 1. In Gilbert's model, errors occur only in the bad state with an emission probability $P_E > 0$. Assuming that in time instance n the model is in the bad state, a biased coin is tossed to produce the n th observed digit, which could be either 1 (with probability P_E) representing a packet error event or 0 (with probability $1 - P_E$) representing a successful packet transmission. After a digit is produced, a state transition takes place. This transition is governed by the probabilities of changing from the bad to the good state (P_{BG}) and from the good to the bad state (P_{GB}). After the state transition, the $(n+1)^{th}$ digit is produced. Thus, given the current state, the current digit of the error pattern is independent of all previous digits. Carefully note that a biased coin is only tossed for generating observation digits in the bad state, since the good state is error-free. Therefore, if an observed digit of the error pattern is a 1, it is clear that the process is in the bad state. On the other hand, observing a 0 does not tell us whether the underlying state is good or bad. Therefore, the Gilbert model is a model with hidden or unobserved states. We further note that the states of Gilbert's model are persistent, i.e., $P_{BG} \ll 1 - P_{BG}$, $P_{GB} \ll 1 - P_{GB}$, and therefore the resulting error patterns have a burst structure.

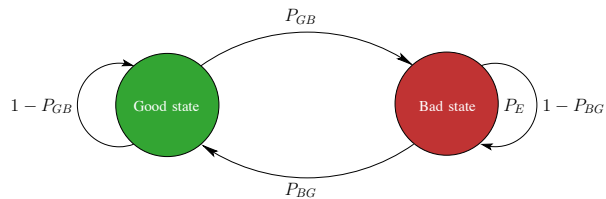


Fig. 1: Schematic illustration of the Gilbert model.

We propose to use Gilbert's model to statistically describe the measured V2I packet error patterns. However, since the performance of such communication links strongly depends on the distance between the transmitter and the receiver due to propagation effects and interference, a simplistic two-state model with constant parameters should not be used in order to avoid a loss of important channel effects. To maintain an accurate representation of the propagation effects and interference in the measurement data, we divide each measurement into N parts corresponding to N disjoint distance intervals of the same length. The transition probabilities (P_{BG} , P_{GB}) and the emission probability (P_E) are estimated separately for each interval using the Baum-Welch algorithm [13]. Once the model parameters for all N intervals are estimated, we can combine them as shown in Fig. 2 to form a range-dependent modified Gilbert model. This model retains all properties of the original Gilbert model, except for the fact that the model parameters (P_{BG} , P_{GB} , P_E) change as soon as the vehicle leaves the current interval. The initial model state is randomly chosen, while for all subsequent intervals the initial state is equal to the final state in the previous interval.

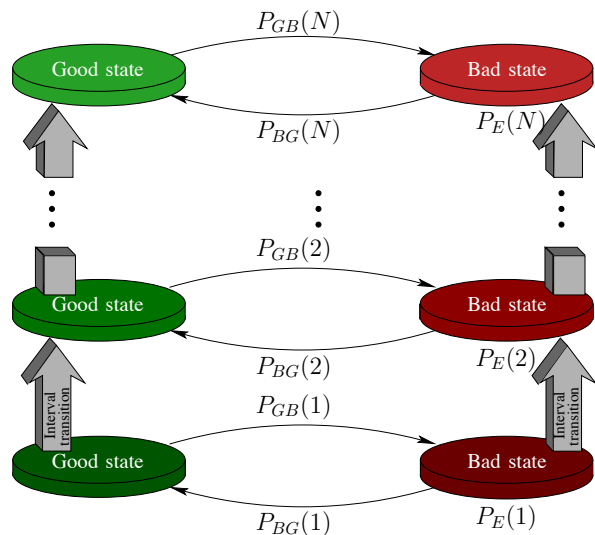


Fig. 2: Schematic illustration of the proposed range-dependent modified Gilbert model.

Clearly, the choice of the granularity, i.e., the length of the interval in which the model parameters do not change,

is essential for the accuracy of our range-dependent modified Gilbert model. On the one hand, the granularity cannot be chosen arbitrarily small since dividing the measured error pattern into very short intervals will destroy the statistics of the data used to estimate the model parameters. On the other hand, estimating the model parameters for large intervals inevitably averages out the local behavior of the propagation channel, e.g., small-scale fading. Therefore, a crucial question that arises when approximating the measured packet error random process with a model, is how to select the granularity. In order to quantify how good the approximation is for a given granularity, we first convert the error patterns to a packet delivery ratio (PDR). The PDR is defined as the number of error-free packets divided by the number of detection events in a time interval $T = \Delta d/v$. To calculate the PDR as a function of the distance, we compute a moving average of the corresponding error pattern where we set Δd to 10 m and v is the velocity of the test vehicle, which we obtain from GPS data. We note that the PDR values are real numbers between 0 and 1, whereas the error pattern consists only of zeros and ones. Next, we estimate the probability distribution of the measured and modeled PDR values using histograms with K bins, yielding K probabilities p_i and q_i , $i = 1, 2, \dots, K$, respectively. Finally, we compute the distance between these probability distributions in terms of the Kullback-Leiber (KL) divergence (also known as relative entropy among information theorists). The KL divergence is calculated as follows:

$$D_{KL}(p||q) = \sum_i p_i \log_2 \frac{p_i}{q_i}$$

Loosely speaking, the KL divergence $D_{KL}(p||q)$ measures the information loss when using the approximate distribution q rather than the true distribution p . We note that $D_{KL}(p||q)$ is always nonnegative and $D_{KL}(p||q) = 0$ if and only if $p = q$. The KL divergence between the measured and modeled PDR distributions with granularities from 1 m to 150 m is shown in Fig. 3. As expected, a better approximation of the measurement can be achieved by estimating the model parameters with smaller granularities. Granularities below 10 m do not yield a significant decrease of the KL divergence, while considerably increasing the number of intervals and thereby boosting the computational overhead of our model.

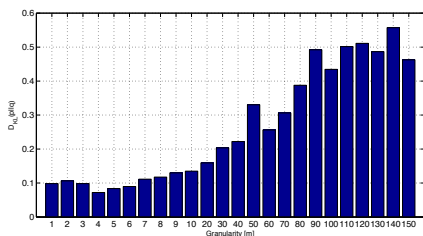
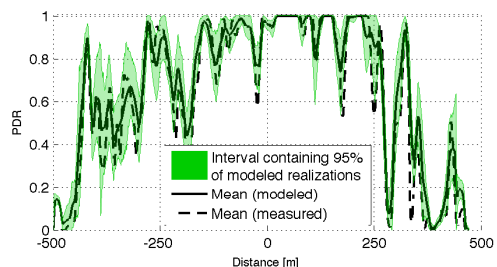


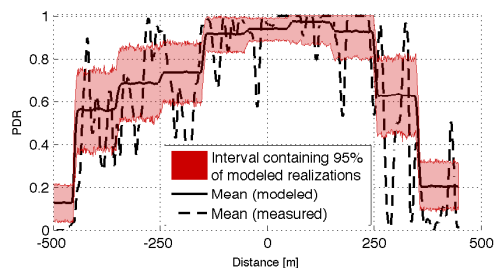
Fig. 3: KL divergence between the measured and modeled PDR distributions with granularities from 1 m to 150 m.

For a better perception of this result we compare the PDR values obtained from measurements with the PDR values

generated by our model with a granularity of 10m and 100m, shown in Fig. 4(a) and 4(b), respectively. The curves are plotted versus the distance d , where the origin of the abscissa ($d = 0$ m) corresponds to the position of the RSU. Negative values on the abscissa correspond to locations where the vehicle was approaching the RSU and positive distances represent the vehicle locations after passing the RSU. The solid and dashed lines show the average PDR for modeled and measured traces, respectively. We have generated 1000 realizations using our model and the colored bands in Fig. 4 represent the intervals in which 95% of all realizations lie. We note that for the model with smaller granularity these 95% intervals are very small, i.e., almost all realizations approximate the measurement result very well. In contrast, the 95% intervals for the model with greater granularity are significantly larger and we obtain the average performance in 100m steps, corresponding to the model granularity. This is not surprising, since the model parameters were estimated using data blocks, which are significantly longer than the coherence time of the channel. We note that the 95% intervals are not the confidence intervals of the mean values. In fact, the confidence intervals of the mean values would be almost indistinguishable from the solid lines in Fig. 4. Finally, we note that despite the dependence of the PDR on the model granularity, our previous results [14] have shown that all key performance indicators (KPIs) could be closely reproduced by our model for a wide range of granularities.



(a) Results of model with granularity of 10 m.



(b) Results of model with granularity of 100 m.

Fig. 4: Empirical intervals containing 95% of all realizations for PDR calculated based on modeled traces. Solid and dashed lines show PDR average for 1000 model realizations and 10 measurement repetitions, respectively.

We conclude that the granularity of the proposed model can be used to achieve a trade-off between approximation accuracy and model complexity and, hence, the granularity should be chosen according to the application-specific requirements. In this work, our aim is to produce very accurate models for specific measurement equipment, transmission parameters and propagation environment and therefore, we hereafter use the range-dependent modified Gilbert model with granularity of 10m.

III. EXPERIMENTAL SETUP

In order to obtain the real-world reference data for modeling the packet error behavior of V2I systems, we have conducted an extensive series of measurements on the highway S1 in Austria. The measurements were performed at a center frequency of 5.9GHz with real vehicular traffic patterns. The average test vehicle speed was 80 km/h (22.2 m/s) with marginal deviations due to traffic. In our measurements we have used a single OBU receiver and a single RSU transmitter. There were no other interfering transmitters along the test track.

As OBU receiver we have used the cooperative vehicle-infrastructure systems (CVIS) platform [15], equipped with a radio module implementing the IEEE 802.11p protocol and a GPS receiver constantly logging the exact position of the device. The OBU receiver was connected to the OBU antenna, which has been mounted using magnets on the roof of our test vehicle (a Ford Galaxy) at a height of approximately 1.7 m. As OBU antenna the CVIS vehicle rooftop antenna was used. The CVIS CALM M5 antenna is a vertically polarized broadband (2.06.7 GHz) double-fed printed monopole with a radiation pattern close to omnidirectional. The antenna performance is 5 dBi (peak gain).

As RSU transmitter we have used another unit of the CVIS platform, featuring the same characteristics as the OBU receiver. The transmitter platform was placed inside a weather protection cabinet close to a highway gantry, where it has been connected to the mains and a local area network. The radio front-end of the IEEE 802.11p transceiver was connected via a 3 dB power splitter to a set of two identical directional antennas. The antennas were mounted on the highway gantry, 7.1 m above the road and were pointing along both driving directions to ensure homogenous coverage. Detailed antenna characteristics and mounting positions are given in Table I.

While the RSU was transmitting constantly in broadcast mode with data rates and packet lengths as specified in Table I, the OBU was recording within the expected coverage range, i.e., approximately 500 m before and after passing the RSU location. We note that throughout the measurement campaign there was no uplink signaling of any kind. The transmitter and the receiver were communicating in the so-called outside

the context of a basic service set (OCB) mode, thus avoiding latency caused by channel scanning, authentication and association phases.

For each detection event (captured using the open source protocol analyzer Wireshark) the OBU recorded time and location as provided by the GPS receiver together with the received signal strength indicator (RSSI) estimated by the CVIS radio module. For the purpose of accurate RSSI estimation, the equipment was carefully calibrated through a series of lab measurements. All detection events undergo a cyclic redundancy check (CRC) used to determine whether the detected packet has been decoded correctly or not. Based on the result of the CRC a binary error pattern containing information about all detection events is created. This error pattern together with the GPS data is used for performance evaluation in the post-processing phase.

A. Key Performance Indicators

To enable comparability of V2I measurements with different parameter settings, equipment and driving directions, we define a set of KPIs. As basis for the calculation of the KPIs we use the PDR as a function of the absolute distance between OBU and RSU, which will serve as an illustrative comparison in what follows. An example is shown in Fig. 5. Here the PDR at absolute distance d is computed by averaging the PDR values in the intervals $[-d - \Delta/2, -d + \Delta/2]$ and $[d - \Delta/2, d + \Delta/2]$, with $\Delta = 10$ m.

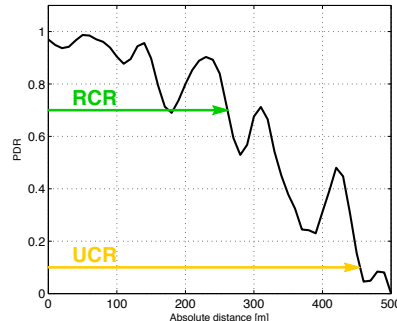


Fig. 5: Definition of RCR and UCR, based on the PDR as a function of absolute distance from the RSU.

The KPIs are defined as follows:

- Reliable connectivity range (RCR), introduced in [9] is the range over which high quality communications can be established. It is defined as the absolute distance from the RSU, such that the PDR values are greater than 0.7 as shown by the green arrow in Fig. 5. As shown by this example in some measurements the PDR drops below the threshold of 0.7 several times. For these cases we define a sub-threshold of 0.5 and define the RCR as the distance at which the PDR is larger than 0.7 for the last time before dropping below 0.5. We also note, that for certain operation modes the PDR values in the close vicinity of (or directly under) the RSU are below the

¹Equivalent isotropically radiated power (EIRP) comprises antenna gain, cable losses and transmit power. Transmit power was set to 10 dBm in all setups except 7 and 8.

²Right-handed circular polarization (RHCP).

TABLE I: Detailed description of the 12 different measurement setups.

	Packet length [Byte]	Data rate [Mbit/s]	Driving direction	Antenna position	Antenna gain [dBi]	EIRP ¹ [dBm] / [mW]	3 dB beamwidth hor.ver. [°]	Polarization
Setup 1	200	6	on RSU lane	on highway side	10	16.8/47.9	35/35	RHCP ²
Setup 2	1554	6	on RSU lane	on highway side	10	16.8/47.9	35/35	RHCP
Setup 3	200	12	on RSU lane	on highway side	10	16.8/47.9	35/35	RHCP
Setup 4	200	6	on opposite lane	on highway side	10	16.8/47.9	35/35	RHCP
Setup 5	1554	6	on opposite lane	on highway side	10	16.8/47.9	35/35	RHCP
Setup 6	200	12	on opposite lane	on highway side	10	16.8/47.9	35/35	RHCP
Setup 7	200	6	on RSU lane	middle of highway	14	12.2/16.6	40/30	vertical
Setup 8	200	6	on opposite lane	middle of highway	14	12.2/16.6	40/30	vertical
Setup 9	200	6	on RSU lane	on highway side	6	12.8/19.1	60/60	RHCP
Setup 10	200	6	on opposite lane	on highway side	6	12.8/19.1	60/60	RHCP
Setup 11	200	6	on RSU lane	on highway side	13	19.8/95.5	42/23	RHCP
Setup 12	200	6	on opposite lane	on highway side	13	19.8/95.5	42/23	RHCP

threshold of 0.7. These PDR values are excluded for the RCR calculation.

- Unreliable communication range (UCR), introduced in [9] is the distance at which the PDR drops below 0.1 for the first time shown in Fig. 5 by the yellow arrow. Therefore, for $RCR \leq |d| \leq UCR$ we cannot guarantee reliable communication quality, which is, however, not required by all vehicular communications applications.
- Throughput is the total number of packets successfully decoded during one measurement multiplied by the packet length in Byte.
- Error fraction is the percentual relationship of lost or erroneously decoded packets to the total number of transmitted packets during one measurement.

IV. COMPARATIVE ANALYSIS OF SYSTEM PERFORMANCE

We next summarize real-world measurement-based performance results of V2I communications. In what follows, all results are averaged over 1000 realizations of our range-dependent modified Gilbert model with a granularity of 10 m. The model parameters were estimated based on a sufficiently large number of measurement runs. The main advantages of this approach are twofold: On the one hand, it improves the reliability of the results due to the significantly increased number of realizations and on the other hand it enables full reproducibility of the experiments using the publicly available model parameters [11].

TABLE II: Summary of experimental results.

	RCR [m]	UCR [m]	Throughput [Mbits]	Error fraction [%]
Setup 1	268	490	8.14	23.4
Setup 2	253	470	14.28	27.2
Setup 3	150	330	7.62	42.8
Setup 4	385	480	7.29	25.5
Setup 5	250	480	12.18	32.5
Setup 6	100	410	5.91	53.2
Setup 7	173	390	4.33	40.8
Setup 8	171	370	4.11	41.4
Setup 9	91	290	3.53	35.7
Setup 10	84	280	3.53	32.4
Setup 11	250	480	7.33	28.7
Setup 12	230	470	6.63	24.1

A. Experiment 1: Data rate versus packet length for system throughput boosting

The objective of this experiment is to find a set of system parameters yielding the largest throughput using a constant transmit power of 10 dBm. One possible approach is to increase the packet length, thus decreasing the total amount of non-payload overhead. Here, the main disadvantage is the deterioration of the preamble-based channel estimates due to the increased transmission time. This is especially true

in highly time-variant vehicular propagation environments. Furthermore, for a given bit error probability it is more likely to observe a bit error, and thus a packet error (detected by the CRC), in a longer packet. Therefore, we expect that the error fraction will grow with increasing packet length. Another possibility to achieve higher throughput is to use higher data rates. In this case the time required to transmit a packet will be reduced, resulting in an improved quality of channel estimates.

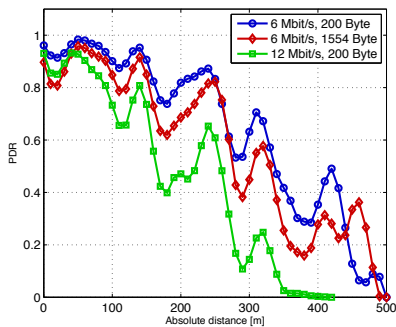


Fig. 6: PDR performance of systems transmitting with 6 Mbit/s & 200 Byte (blue), 6 Mbit/s & 1554 Byte (red), 12 Mbit/s & 200 Byte (green).

To check these claims we have performed experiments with setup 1, 2, and 3 considering packet lengths of 200 Byte and 1554 Byte (corresponding to the maximum packet length supported by the CVIS transmitter) and data rates of 6 Mbit/s (QPSK with code rate 1/2) and 12 Mbit/s (16 QAM with code rate 1/2). For these setups, the average PDR performance versus the absolute distance from the RSU is shown in Fig. 6. By inspection of the plots it becomes evident that both the packet length extension and the increased data rate lead to performance degradation in terms of packet reception probability for a given distance from the RSU. Table II shows that not only the PDR, but also the coverage range was reduced for both settings. However, coverage range reduction due to use of longer packets is rather marginal and amounts to 5.6% and 4% for RCR and UCR, respectively. In contrast, the RCR was reduced by 44% and the UCR by 33% when doubling the data rate. The error fraction was increased by 4% and 19.4% for longer packets and higher data rate, respectively. However, it was possible to increase the throughput by 75.4% for setup 2 while for setup 3 the throughput was reduced by 6.4%.

We conclude that in contrast to our initial expectations, shortening the packet duration by using a higher-order modulation scheme resulted in an overall performance degradation instead of a throughput increase. This result can be explained as follows:

- The RSU antenna in the considered setups was mounted high above the vehicles, yielding a strong line-of-sight component and therefore rendering the underlying V2I channel less time-variant than a typical V2V channel. Thus the well-investigated dependence between packet length and channel estimation accuracy becomes less

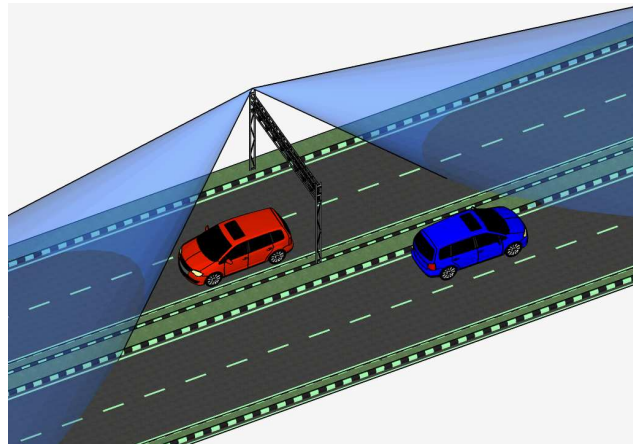


Fig. 7: Schematic representation of the RSU mounting position for setups 1-6. Here, the red vehicle is driving on the RSU lane and the blue vehicle is driving on the opposite lane.

pronounced.

- The use of higher-order modulation schemes imposes increased SNR requirements. Since for a given SNR value, the constellation symbols are spaced more closely the higher the modulation order is.

B. Experiment 2: Influence of the driving direction for systems with different parameter settings

This experiment corresponds to the measurement setups 4, 5, and 6. We compare the influence of the driving direction on the system performance with different parameter settings. The position of the RSU antenna in relation to the road geometry is schematically shown in Fig. 7, where the blue and red vehicle represents the test vehicle driving on the RSU lane and on the opposite lane, respectively. The PDR plots for different parameter settings are shown in Fig. 8, with red and blue representing the average performance on the RSU lane (setups 1 - 3) and on the opposite lane (setups 4 - 6), respectively. Comparing these results, it becomes evident that the influence of the driving direction on the system performance becomes more pronounced at higher data rates (cf. Fig. 8(c)). Particularly, the RCR is reduced by 33% due to a change of the driving direction when doubling the data rate, while it remains almost unchanged when using a lower data rate (irrespective of the packet length). Moreover, for higher data rate the throughput was decreased by 22% and the error fraction was increased by 24%. While a change of the driving direction resulted in much smaller performance degradation for lower data rates, namely the throughput was decreased by 10% and the error fraction was increased by 9% for shorter packets and by 15% and 20% for longer packets.

A further remarkable difference when evaluating the influence of the driving direction is the distinctive notch of the PDR values around $0 \leq |d| \leq 30$ m for measurements performed on the opposite lane with all parameters. Our observations suggest that this explicit drop of the PDR in close vicinity of the RSU

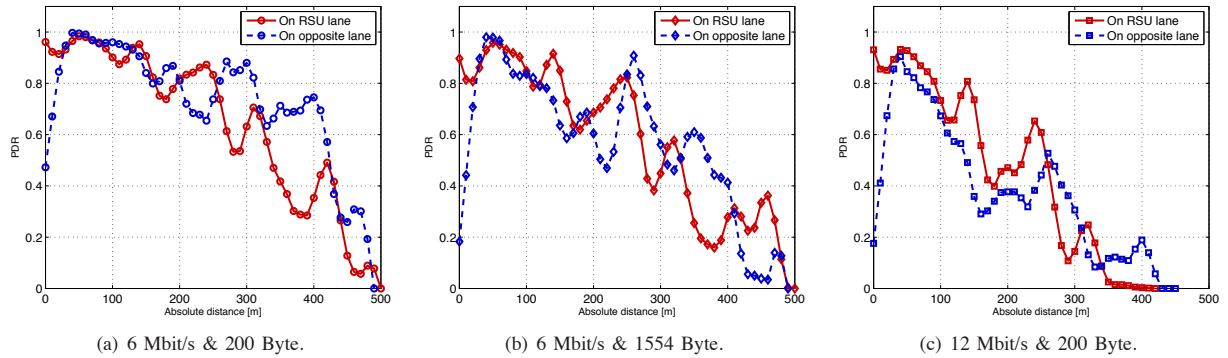


Fig. 8: Influence of the driving direction on the PDR performance for systems with different data rates and packet lengths. The red curves represent measurements on the RSU lane and the blue curves correspond to measurements on the opposite lane.

is due to the specific choice of the RSU antenna type, and, more importantly, due to the antenna mounting position with respect to the road geometry. This claim will be verified in the next experiment.

C. Experiment 3: Optimizing the RSU antenna position to decrease the influence of the driving direction

To show that the performance degradation of V2I communication due to a change of the driving direction is caused by the mounting position of the RSU antenna with respect to the road geometry, we have performed measurements with setup 7 and 8. In this case, the RSU antennas were mounted on the other side of the same highway gantry, exactly between the two driving directions. From Table I, we can see that not only the mounting position of the antenna, but also the antenna gain has changed. Since the antennas used in setups 7 and 8 have a higher gain than those in setups 1 through 6, we had to reduce the transmit power to obtain comparable EIRPs. The schematic comparison of the antenna radiation pattern for measurement setups 1 through 6 versus measurements setups 7 and 8 is shown in Fig. 9 in blue and yellow, respectively. We clearly see that with the new setup, the signal is radiated more homogeneously along the highway and the coverage areas for both driving directions are more alike than for the setups 1 through 6. Particularly, while the red vehicle on the RSU side has coverage for both mounting positions, the blue vehicle driving on the opposite lane can only be served by the RSU with antennas mounted in the middle of the highway, although the distance to the highway gantry is the same for both driving directions.

Fig. 10 highlights the influence of the driving direction in systems with RSU antennas mounted in the middle of highway. Comparing the blue and the red curves we notice that the notch around the origin of the abscissa is not present anymore (cf. Fig. 8), while both the RCR (1% less for opposite lane) and the UCR (5% less for opposite lane) remain almost unchanged. The total throughput loss due to a change of the driving direction is only 5% and the error fraction remains nearly unchanged. This marginal performance loss obtained

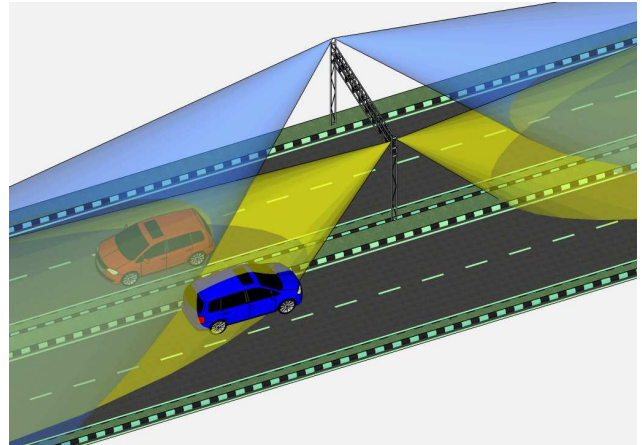


Fig. 9: Schematic representation of the RSU mounting position. Blue and yellow colors represent the antenna on the side (setups 1-6) and in the middle of the highway (setups 7&8), respectively.

for measurements on the opposite lane is due to a minor inaccuracy of the RSU antenna alignment.

We conclude that not the change of the driving direction itself, but rather the mounting position of the RSU antennas has a significant impact on the performance, especially when higher data rates are used. Based on this experiment, we suggest to mount RSU antennas in the middle of the highway, rather than on one side to avoid undesirable performance degradation.

D. Experiment 4: Benefits and drawbacks of RSU antenna gain increase

Although it was possible to nearly eliminate the influence of the driving direction on the system performance when using setups 7 and 8 instead of setups 1 and 4, a quantitative comparison of the KPIs shows that the overall performance was worse when we increased the RSU antenna gain while decreasing the transmit power. Therefore, in this final experiment we study

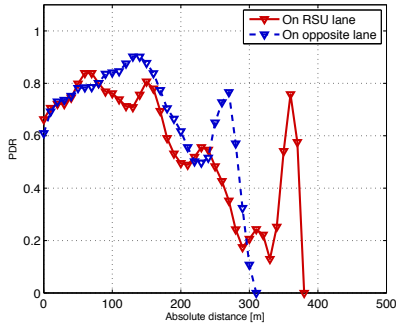


Fig. 10: Influence of driving direction on the PDR performance for systems with RSU antenna mounted in the middle of highway.

the dependence of the system performance on the RSU antenna gain.

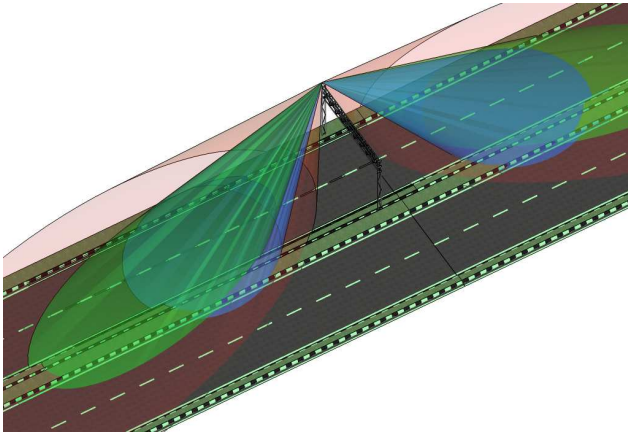
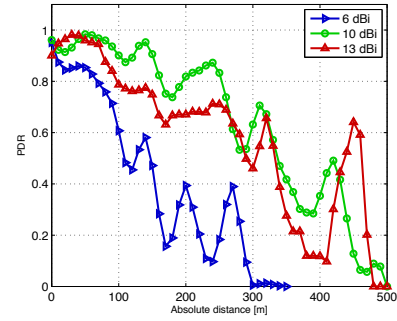


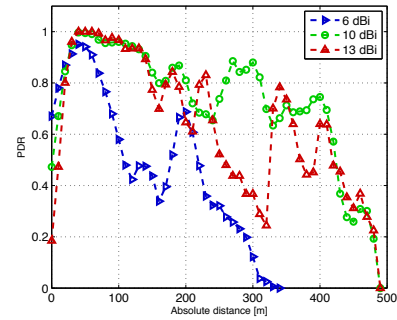
Fig. 11: Schematic comparisons of radiation patterns for RSU antennas. Blue, green and red colors represent antennas with gain of 6 dBi (setups 9 & 10), 10 dBi (setups 1-6) and 13 dBi (setups 11 & 12), respectively.

To this end, in addition to the RSU antennas used in setups 1 through 6, we have used antennas with smaller and larger gain corresponding to setups 9, 10 and 11, 12, respectively. Three antennas with different gains were mounted in the same antenna unit, ensuring an identical mounting position for each setup. The transmit power was constant for all setups, corresponding to different EIRP values, as schematically shown in Fig. 11.

Comparing the PDR plots for measurements with different RSU antenna gains (cf. Fig. 12), we can conclude that the best performance was achieved when using RSU antennas with a gain of 10 dBi, since the green curve lies strictly above the red and the blue curves for both driving directions. The 4 dBi decrease of the RSU antenna gain (blue curves in Fig. 12) resulted in a significant decrease of RCR and UCR by 66% and 40%, respectively. The throughput was decreased by 57% and up to 13% more transmitted packets



(a) On RSU site.



(b) On opposite lane.

Fig. 12: PDR performance for systems with RSU antenna gain of 6 dBi (blue), 10 dBi (green), and 13 dBi (red).

were decoded erroneously. Thus, it is possible to nearly double the throughput and coverage when investing additionally 4 dBi in RSU antenna gain. However, an antenna gain increase by further 3 dBi (red curves in Fig. 12) did not yield a proportional performance enhancement. In contrast to our expectation, both the RCR and the throughput were reduced by 7% and 10%, respectively. The qualitative relation of measurements with different RSU antenna gains for opposite driving direction remains unchanged.

We anticipate that using antennas with higher gains, e.g., 10 dBi instead of 6 dBi, can considerably increase the overall performance of systems with directional RSU antennas. However, this performance improvement is not strictly proportional to the antenna gain, since with increasing antenna gain the requirements with respect to precise antenna positioning and alignment are increasing as well.

V. CONCLUSION

We propose a computationally low-cost range-dependent modified Gilbert model that allows to accurately reproduce the packet error statistics of real-world wireless V2I links. The model parameters have been estimated using data acquired during an extensive IEEE 802.11p V2I field-testing campaign. We then simulated a large number of model-generated data traces to numerically evaluate the impact of communication settings and RSU deployment conditions on the link performance. The obtained results indicate that using longer packets

is more suitable than using higher data rates to increase the throughput of V2I communications. Moreover, our measurement results reveal a strong influence of the driving direction (notably nearby the RSU) for higher data rates. To reduce the performance differences between both driving directions, we recommend to carefully choose the RSU antenna mounting position and configuration with respect to the road geometry. Specifically, we recommend the use of high-gain directional RSU antennas mounted on a highway gantry in between both driving directions. An increase of the antenna gain, however, does not directly translate into a performance increase, since the use of high-gain directional RSU antennas imposes high requirements on the antenna positioning and placement. The complete set of model parameters is publicly released to facilitate future system-level performance evaluations of cooperative vehicular communication systems.

ACKNOWLEDGMENT

This work was performed with partial support by the Christian Doppler Laboratory for Wireless Technologies for Sustainable Mobility and the ROAD-SAFE project, a scientific cooperation between FTW, TU Wien, ASFINAG Maut Service GmbH, Kapsch TrafficCom AG and Fluidtime GmbH. We acknowledge the Federal Ministry for Transport, Innovation, and Technology of Austria (BMVIT) for granting a test license in the 5.9GHz band. We further appreciate support of COST Action IC1004 on cooperative radio communications for green smart environments.

REFERENCES

- [1] A. Böhm, K. Lidström, M. Jonsson, and T. Larsson, "Evaluating calm m5-based vehicle-to-vehicle communication in various road settings through field trials," in *Local Computer Networks (LCN), 2010 IEEE 35th Conference on*, 2010, pp. 613–620.
- [2] R. Meireles, M. Boban, P. Steenkiste, O. Tonguz, and J. Barros, "Experimental study on the impact of vehicular obstructions in vanets," in *Vehicular Networking Conference (VNC), 2010 IEEE*, 2010, pp. 338–345.
- [3] V. Shivaldova, G. Maier, D. Smely, N. Czink, A. Paier, and C. F. Mecklenbräuker, "Performance analysis of vehicle-to-vehicle tunnel measurements at 5.9 GHz," in *General Assembly and Scientific Symposium of International Union of Radio Science (URSI)*, August 2011.
- [4] B. Gallagher, H. Akatsuka, and H. Suzuki, "Wireless communications for vehicle safety: Radio link performance and wireless connectivity methods," *Vehicular Technology Magazine, IEEE*, vol. 1, no. 4, pp. 4–24, 2006.
- [5] S. Dickey, C.-L. Huang, and X. Guan, "Field measurements of vehicle to roadside communication performance," in *Vehicular Technology Conference, 2007. VTC-2007 Fall. 2007 IEEE 66th*, 2007, pp. 2179–2183.
- [6] A. Paier, R. Tresch, A. Alonso, D. Smely, P. Meckel, Y. Zhou, and N. Czink, "Average downstream performance of measured IEEE 802.11p infrastructure-to-vehicle links," in *2010 IEEE International Conference on Communications (ICC 2010)*, May 2010.
- [7] M. Shulman and R. Deering, "Third annual report of the crash avoidance metrics partnership april 2003–march 2004," Nat. Highw. Traffic Safety Admin. (NHTSA), Washington, DC, January 2005.
- [8] A. Paier, D. Faetani, and C. F. Mecklenbräuker, "Performance evaluation of IEEE 802.11p physical layer infrastructure-to-vehicle real-world measurements," in *Third International Symposium on Applied Sciences in Biomedical and Communicational Technologies (ISABEL)*, November 2010.
- [9] J. Gozalvez, M. Sepulcre, and R. Bauza, "IEEE 802.11 p vehicle to infrastructure communications in urban environments," *Communications Magazine, IEEE*, vol. 50, no. 5, 2012.
- [10] <https://portal.ftw.at/projects/roadsafe>.
- [11] <http://www.nt.tuwien.ac.at/downloads/>.
- [12] E. N. Gilbert, "Capacity of a burst-noise Channel," *Bell System Technical Journal*, vol. 39, no. 9, pp. 1253–1265, 1960.
- [13] L. E. Baum, T. Petrie, G. Soules, and N. Weiss, "A Maximization Technique Occurring in the Statistical Analysis of Probabilistic Functions of Markov Chains," *The Annals of Mathematical Statistics*, pp. 164–171, 1970.
- [14] V. Shivaldova and C. F. Mecklenbräuker, "A Two-State Packet Error Model for Vehicle-to-Infrastructure Communications," in *78th IEEE Vehicular Technology Conference, 2013*, September 2013.
- [15] <http://www.cvisproject.org>.